Phase separation of photogenerated carriers and photoinduced superconductivity in high-T_c materials

G. Yu, C. H. Lee, and A. J. Heeger
Institute for Polymers and Organic Solids, University of California, Santa Barbara, Santa Barbara, California 93106

N. Herron and E. M. McCarron
E. I. du Pont de Nemours and Co., Inc., Central Research and Development Department, Wilmington, Delaware 19898

Lin Cong, G. C. Spalding, C. A. Nordman, and A. M. Goldman
Center for the Science and Application of Superconductivity, University of Minnesota, Minneapolis, Minnesota 55455
(Received 29 July 1991; revised manuscript received 24 October 1991)

The temperature dependences of the transient photoinduced conductivity *at different light levels* in single crystals of $YBa_2Cu_3O_{7-\delta}$ and ultrathin (~40-Å) epitaxial films of $DyBa_2Cu_3O_{7-\delta}$ *with fixed* δ are qualitatively and quantitatively similar to those of the doping-induced conductivity in $YBa_2Cu_3O_{7-\delta}$ and $DyBa_2Cu_3O_{7-\delta}$ *with different oxygen content* δ, indicative of "photodoping" over a wide range of resistivities. Signatures of the photoinduced transition to metallic behavior are observed at light intensities greater than 10^{15} photons/cm^2. At these high levels of photoexcitation, the thermal activation energy approaches zero and a minimum appears in the temperature dependence of the photoresistivity below 100 K. The resistivity minimum, reminiscent of the onset of superconductivity in inhomogeneous samples and in granular superconductors, is interpreted in terms of a phase separation of the photogenerated carriers and metallic-droplet formation subsequent to photoexcitation. A modest longitudinal magnetic field (≤ 0.5 T) reduces both the resistivity minimum and the superlinear contribution to the transient photoconductance. For oxygen levels close to the metal-insulator transition ($\delta \approx 0.6$), the lifetime of the photoexcited state is enhanced by nearly three orders of magnitude at high excitation levels, indicative of metastability.

I. INTRODUCTION

Although many aspects of the phenomena of high-temperature superconductivity (HTSC) in the layered cuprates remain unexplained, the transition from the insulating and antiferromagnetic phase to the metallic and superconducting phase is known to be correlated with the density of charge carriers in the CuO_2 planes. Following the initial discovery by Bednorz and Müller,[1] considerable effort has been focused on the ability to control the carrier density n_c by chemical doping, either by mixed-valence substitution, as in $La_{2-x}Sr_xCuO_4$ and $Bi_2Sr_2Ca_{1-x}Y_xCu_2O_8$, or by variation of the oxygen content (δ), as in $YBa_2Cu_3O_{7-\delta}$.[2] Photoexcitation offers an attractive alternative method to vary the concentration of charge carriers with a number of advantages; for example, n_c can be increased without the added complication of a change in chemical composition and crystal structure, and n_c can be increased in a transient manner with subnanosecond resolution using pulsed-laser techniques. The former is important for it allows one to study the system as a function of n_c without simultaneously changing the degree of disorder; the latter is important for it provides one with the opportunity to probe the dynamics of the electronic system at short times and well away from equilibrium.

The initial results of transient photoinduced-conductivity measurements in semiconducting single crystals of $YBa_2Cu_3O_{6.3}$ indicated that the magnitude of the peak photocurrent changes dramatically as a function of the light intensity (I_L); the linear dependence at low light intensity becomes first sublinear and then superlinear as a function of I_L.[3] The critical I_L for the onset of this superlinearity is about 5×10^{15} photons/cm^2.

There have been other reports of transient photoconductivity and photoinduced changes in dark conductivity in the insulating "parent" materials of the high-temperature superconductors. Thio *et al.* studied the transient photoconductivity in single crystals of La_2CuO_4 with 10-ns laser-pulse excitation and observed a long-lived photocurrent with a power-law decay.[4] Kirilyuk and co-workers reported that the resistivity of $YBa_2Cu_3O_{7-\delta}$ thin films decreased after extended laser illumination.[5,6] Using a 1-μm-thick $YBa_2Cu_3O_{7-\delta}$ film aged in vacuum at room temperature to an oxygen concentration near the semiconductor-metal transition ($\delta \sim 0.6$), they found that the resistivity decreased with illumination time; for example, after 20 h illumination, the resistance dropped by 30% at 100 K and by four orders of magnitude at 2 K. The dark-conductivity and magnetic-susceptibility data[5,6] obtained from the films after extended illumination are similar to those in films with higher oxygen concentrations. Thus the use of light to influence the properties of this class of materials provides an opportunity that is of scientific interest and of potential technological importance.

In this paper we extend our previous studies[3,7] of subnanosecond transient photoconductivity in semiconducting crystals of $YBa_2Cu_3O_{7-\delta}$ and in ultrathin epitaxial films of $DyBa_2Cu_3O_{7-\delta}$. We find that the temperature dependences of the transient photoinduced conductivity at different light levels in single crystals of $YBa_2Cu_3O_{7-\delta}$ and ultrathin (~ 40 Å) epitaxial films of $DyBa_2Cu_3O_{7-\delta}$ at fixed δ are qualitatively and quantitatively similar to the doping-induced conductivity at different oxygen content, indicative of "photodoping" over a wide range of resistivities. By analyzing the data from $YBa_2Cu_3O_{6.3}$ at different light levels as a function of temperature, we find signatures of the transient photoinduced transition to metallic behavior at light intensities greater than about 5×10^{15} photons/cm^2: (i) The activation energy of the temperature dependence of the photoinduced conductivity σ_{ph} approaches zero; (ii) a minimum appears below 100 K in the temperature dependence of the resistivity, $\rho_{ph}(T)=1/\sigma_{ph}(T)$, where σ_{ph} is the peak transient photoconductivity following photo-excitation.

The minimum in $\rho_{ph}(T)$ at low temperature is reminiscent of the onset of superconductivity in inhomogeneous (mixed-phase) samples and similar to that observed from "local superconductivity" in granular superconductors.[8,9] This borderline metallic behavior is interpreted in terms of intrinsic phase separation of the photogenerated carriers and metallic-droplet formation in the antiferromagnetic insulator subsequent to photoexcitation.[7] Phase separation into metallic regions is consistent with the observation of metastability: At high excitation levels of samples with oxygen content close to the metal-insulator transition ($\delta\approx0.6$), the lifetime of the photoexcited state is enhanced by nearly three orders of magnitude; the photoinduced sheet conductivity persists at the value characteristic of the metal-insulator transition ($\Sigma\sim e^2/h$) for times in excess of 100 ns.[7,10]

By following both the dark and photoinduced conductivities as a function of aging time in ultrathin films (~ 40 Å) of $DyBa_2Cu_3O_{7-\delta}$ in a series of related experiments, we have successfully monitored the transport behavior at different oxygen concentrations on a single sample over the full range from the metallic and superconducting phase to the semiconducting-insulating phase (with the temperature coefficients of the resistivity changing sign from positive in the metallic phase to large negative value in the insulating phase). In the semiconducting phase with δ near 0.6–0.7, behavior similar to that found in single crystals of $YBa_2Cu_3O_{6.3}$ was observed.

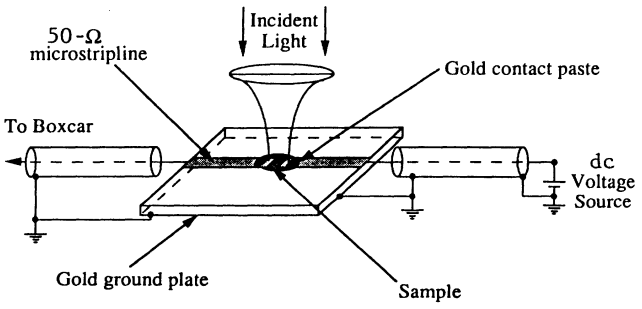

FIG. 1. Schematic diagram of the Auston-switch configuration for fast transient photoconductivity measurements.

The experimental results are discussed in the context of disorder-induced localization and an Anderson-type metal-insulator (M-I) transition in a correlated system in two dimensions.[7] The existence of a minimum metallic sheet conductivity ($\Sigma_{min}\approx e^2/h$) and a corresponding change in the temperature dependence of the resistivity as σ crosses this universal value imply that localization of the charge carriers in the CuO_2 layers due to the random distribution of oxygen at O(1) sites plays an important role in the insulator-metal, or-superconductor transition in the high-T_c cuprates.

II. TRANSIENT PHOTO INDUCED CONDUCTIVITY: EXPERIMENTAL DETAILS

The transient photoconductivity measurement uses the Auston-switch configuration.[11] The sample is mounted across a gap in a 50-Ω stripline transmission line (both the upper strip and ground plane are Au evaporated onto the alumina substrate), as shown in Fig. 1.[3] A dc bias (typically in the range 0–10 V) is applied as indicated. After absorption of a light pulse, the sample acts as a current source; the current pulse propogates down the transmission line into the detector. The 50-Ω impedance matches into the input of the sampling head and boxcar detector, thereby avoiding spurious reflections; the transmission-line configuration enables picosecond temporal resolution (since the configuration is essentially a microwave stripline with >200 GHz frequency response).

The sample-preparation techniques for the $YBa_2Cu_3O_{7-\delta}$ single crystals and $DyBa_2Cu_3O_{7-\delta}$ ultrathin films have been published previously.[3,12] The single-crystal and epitaxial thin-film samples were mounted so that the conductivities were measured in the a-b plane (parallel to the CuO_2 planes). The δ value in the $YBa_2Cu_3O_{7-\delta}$ single crystals is determined by comparison for the x-ray data from the samples used for our experiments[13(a)] to the literature values.[13(b)] The $DyBa_2Cu_3O_{7-\delta}$ epitaxial films had a nominal thickness of ≈ 40 Å (only three to four molecular layers), estimated from the known rates of deposition.[14] With films of this thickness, the optical density is such that only about 10% of the incident photons are absorbed. The different δ values were obtained by progressively aging the $DyBa_2Cu_3O_7$ thin film in a dry (or vacuum) desiccator at room temperature (over periods up to about 2 weeks). Since the oxygen in surface layers of $MBa_2Cu_3O_{7-\delta}$ is unstable when δ is small (here M indicates a rare-earth element such as Y or Dy, etc.[15]), it is relatively easy to control the stoichiometry of a thin film at relevant temperatures. Moreover, by using ultrathin epitaxial films, one can minimize inhomogeneity in the distribution of oxygen across the sample thickness. Such films, therefore, provide a unique opportunity to study the full range of electronic properties from the metallic and superconducting phase to the semiconducting and antiferromagnetic phase with the same sample.

The a-b-plane resistivity $\rho(T)$ in single crystals of

$YBa_2Cu_3O_{7-\delta}$ is thermally activated:

$$\rho(T)=\rho_0 \exp(-E_a/k_B T) . \quad (1)$$

For the $YBa_2Cu_3O_{6.3}$ crystals, the resistivity is about 5×10^2 Ω cm at 300 K, increasing to 1.5×10^{10} Ω cm at 80 K with $E_a=0.18$ eV (at lower temperatures, the temperature dependence deviated from the simple activated form consistent with the resistivity becoming dominated by variable-range hopping). The *a-b*-plane resistivity of the $YBa_2Cu_3O_{6.4}$ crystals is about 10 Ω cm at 300 K, and E_a is nearly an order of magnitude smaller ($E_a=0.03$ eV). After storing the $YBa_2Cu_3O_{6.3}$ crystals in a dry desiccator for more than a year, the activation energy for $YBa_2Cu_3O_{6.3}$ increased from 0.18 to 0.22 eV, indicating of a slight loss of oxygen. All aspects of the photoinduced conductivity data were checked on a number of single crystals of $YBa_2Cu_3O_{7-\delta}$ and on several ultrathin films of $DyBa_2Cu_3O_{7-\delta}$ and were found to be reproducible from sample to sample.

For most experimental results reported in this paper, the excitation source was a N_2 laser with photon energy of 3.7 eV and pulse width of 600 ps. We also present selected data obtained by using 30-ps-pulse-width excitation from a pumped dye laser operating at 2.6 eV. In time-evolution measurements, the gate width of the boxcar (EG&G PARC 4400 system) was selected at 20 ps for the photocurrent measurements at times less than 10 ns. In this case the rise time of the photocurrent resulted from the response of the overall system: approximately 75 ps when pumping with the dye laser and approximately 400 ps when pumping with the N_2 laser. For the time-evolution measurements in the regime from 10 ns to 10μs, the gate width is chosen to be from 2 to 5 ns.

III. TRANSIENT PHOTOINDUCED CONDUCTIVITY: EXPERIMENTAL RESULTS

A. Time profile of the photo-induced conductivity of $YBa_2Cu_3O_{6.3}$

The time profile of the transient photoconductive signal from the Auston switch provides direct information on the time evolution of the photoinduced conductivity. A delay of the maximum photocurrent by about 300–500 ps with respect to the laser excitation pulse was observed in $YBa_2Cu_3O_{6.3}$ and reported previously.[3]

Typical results, obtained with 3.7-eV photons from the N_2 laser (600 ps pulse width, 400 ps instrumental resolution) as pump, are shown in Fig. 2(a) and, with $\hbar\omega=2.6$ eV photons from the dye laser (30 ps pulse width, 75 ps instrumental resolution), are shown in Fig. 2(b). The time delay becomes somewhat larger at the highest light intensity available (this becomes a major effect for $\delta\approx0.6$, indicative of metastability; see Sec. VI). Note that the data in Fig. 2 are quantitative: (i) The photon flux per pulse onto the sample was adjusted to be approximately the same for both the 600-ps excitation pulse (3.7-eV photons) and the 30-ps excitation pulse (2.6-eV photons) so that approximately the same number of photons were absorbed per pulse. (ii) The peak photoconductivity was the same for both the 600-ps excitation pulse and the 30-ps excitation pulse. The fact that the photoconductive response is independent of the time (the pulse width) over which the energy is absorbed demonstrates that the signal is genuine *photoconductivity*, in contrast to that arising from sample heating [which would yield a signal proportional to $I_L\tau^{1/2}=(N/\tau)\tau^{1/2}\sim1/\tau^{-1/2}$, where τ is the pulse width and N is the number of photons deposited during the pulse].[16]

The photoinduced conductivity can be expressed in the form

$$\sigma_{ph}=n_c e\mu , \quad (2)$$

where n_c is the density of photogenerated charge carriers, e is the electron charge, and μ is the carrier mobility. In general, both n_c and μ are time-dependent quantities: The carrier density initially increases during the photoexcitation (or, equivalently, during photoabsorption) and then decays as the photogenerated carriers recombine; $\mu(t)$ can vary as a result of carrier trapping and as a result of the dynamics of the nonequilibrium carrier distribution. *Since there is no delay in photoinduced absorption in*

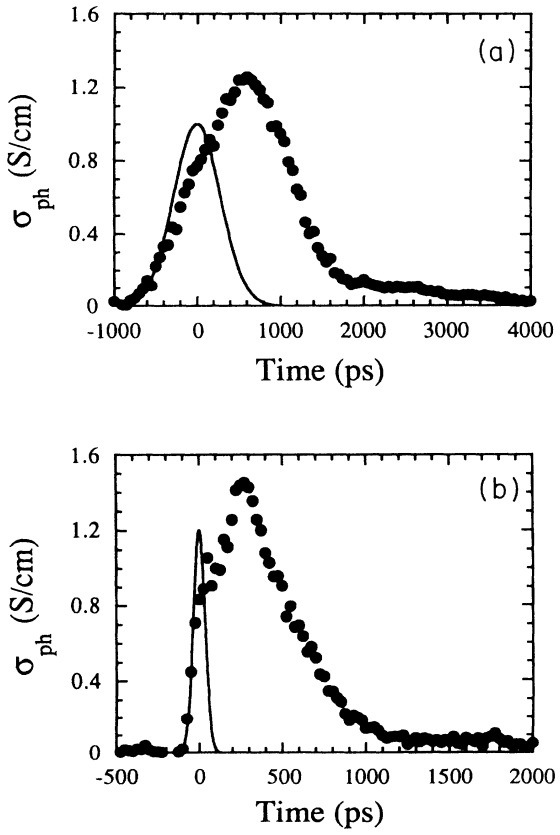

FIG. 2. (a) Typical time evolution of the transient photoconductivity σ_{ph}(●) in $YBa_2Cu_3O_{6.3}$ ($E_a\approx0.18$ eV) under 600-ps, 3.7-eV pulse excitations at 80 K. The photon density is about 7×10^{15} photons/cm^2. (b) Typical time evolution of the transient photoconductivity σ_{ph} (●) in $YBa_2Cu_3O_{6.3}$ ($E_a=0.19$eV) under 30-ps, 2.6-eV pulse excitations at 80 K. The photon density is about 1×10^{16} photons/cm^2. The solid lines in these figure show the positions of the time origins and the time resolution of the overall system obtained from the Gaussian fit of the accompanying weak photovoltaic signals.

$YBa_2Cu_3O_{6.3}$,[17] the time delay of the photoconductance with respect to the photoabsorption, shown in Figs. 2(a) and 2(b), indicates a time delay in the onset of relatively high mobility.

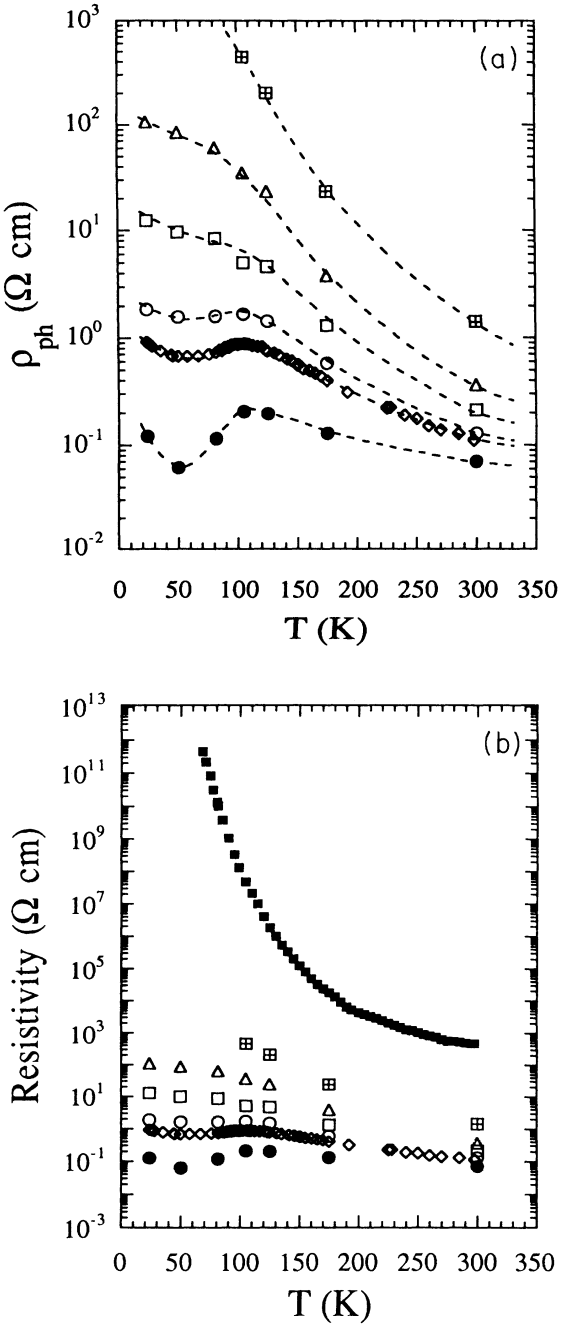

FIG. 3. (a) Temperature dependences of the photoresistivity in $YBa_2Cu_3O_{6.3}$ ($E_a \approx 0.18$ eV), $\rho_{ph}(T)$, at several photon densities; the dashed lines are guides to the eye. $I_L = 1\times10^{13}$ photons/cm^2 (⊞), $I_L = 1\times10^{14}$ photons/cm^2 (△), $I_L = 1\times10^{15}$ photons/cm^2 (□), $I_L = 7\times10^{15}$ photons/cm^2 (○), $I_L = 1.1\times10^{16}$ photons/cm^2 (◇), and $I_L = 2.3\times10^{16}$ photons/cm^2 (●). (b) Temperature dependences of the photoresistivity in $YBa_2Cu_3O_{6.3}$ ($E_a \approx 0.18$ eV), $\rho_{ph}(T)$, at several photon densities compared with the dark resistivity (■) of the same sample.

B. Temperature dependence of σ_{ph}

The temperature dependence of the transient photoinduced resistivity of $YBa_2Cu_3O_{6.3}$, $\rho_{ph}(T)$, is plotted in Fig. 3(a) for several levels of 3.7 eV photoexcitation. The thickness used for the photoinduced-resistivity calculation is chosen as 300 Å, which is inferred from the optical constants.[18] The photoinduced sheet resistance (per molecular layer) can be calculated by dividing the volume resistance by the thickness of the c-axis repeat unit [approximately 12 Å (Ref. 13)]. In Fig. 3(b) the temperature dependences of the photoresistance at successively higher light intensities are directly compared with the dark resistivity in the same sample. The $YBa_2Cu_3O_{6.3}$ data in Fig. 3(b) are replotted on a semilogarithmic scale vs $1/T$; the results are shown in Fig. 4.

The results in Fig. 3 show that, following photoexcitation, the transient photoinduced conductivity can reduce the sample resistivity by many orders of magnitude; the transient decrease in resistivity at 80 K is more than ten orders of magnitude with an incident photon flux of 10^{16} photons/cm^2 ($\sim 3\times10^{21}$ photons/cm^3 in the optical-absorption depth), and this number is even larger at lower temperatures. More importantly, the temperature dependence of the photoinduced resistivity changes dramatically under photo excitation with the following features.

(1) The activation energy decreases as a function of I_L, with $E_a \rightarrow 0$ at $I_L > 5\times10^{15}$ photons/cm^2; this is shown in more detail in Fig. 5.

(2) At high levels of photoexcitation, a minimum appears in $\rho_{ph}(T)$ below 100 K. For $I_L = 2.3\times10^{16}$ photons/cm^2, the minimum value is a factor of 10 below

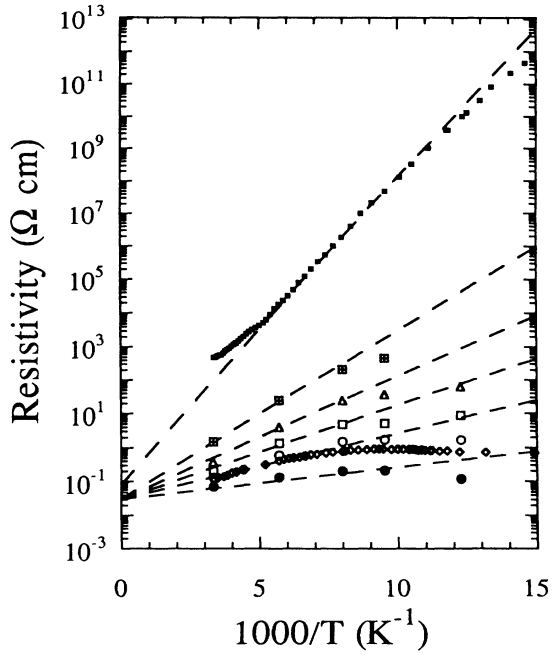

FIG. 4. $\rho_{ph}(T)$ for $YBa_2Cu_3O_{6.3}$ at various levels of photoexcitation are replotted from Fig. 3(b); the symbols and I_L values correspond to those used in Fig. 3. The dashed lines are obtained by fitting the high-temperature data to Eq. (1).

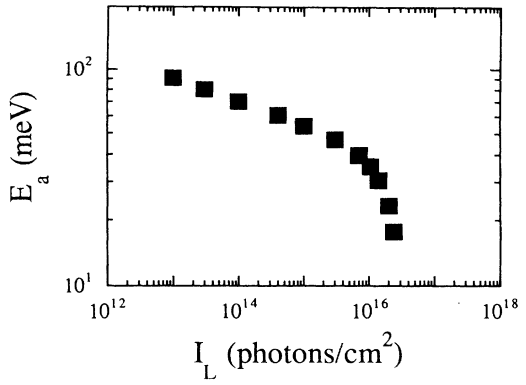

FIG. 5. Activation energy (obtained from slopes of $\log_{10}\rho_{ph}$ vs $1/T$, as in Fig. 4) of the transient photoresistivity in the same sample as that in Fig. 3 is plotted as a function of light intensity. The activation energy of the dark conductivity in this sample is about 0.18 eV.

the value extrapolated from $\rho_{ph}(T)$ above 100 K. This borderline metallic-superconducting feature appears only at photon fluxes of 5×10^{15} cm^{-2} and above.

The instability of oxygen in the surface layers of single crystals of MBa$_2$Cu$_3$O$_{7-\delta}$ (M=Y, Dy, etc.) when δ is small offers an opportunity to alter and control the stoichiometry of ultrathin films.[14] In Fig. 6 we plot the *dark resistivity* of a DyBa$_2$Cu$_3$O$_{7-\delta}$ film as a function of temperature for a number of oxygen concentrations spanning the full range from the metallic and superconducting phase to the insulating antiferromagnetic phase. The different oxygen concentrations were obtained by aging the film at room temperature between the successive measurements of $\rho(T)$. In the inset of Fig. 6, the resistivity versus temperature of the fresh DyBa$_2$Cu$_3$O$_{7-\delta}$ sample, with $\delta\approx0$, is plotted on a linear scale; the onset of the superconducting transition appears at about 80 K. More detailed experimental studies show that zero resistivity in similar films is achieved at 40–50 K.[14]

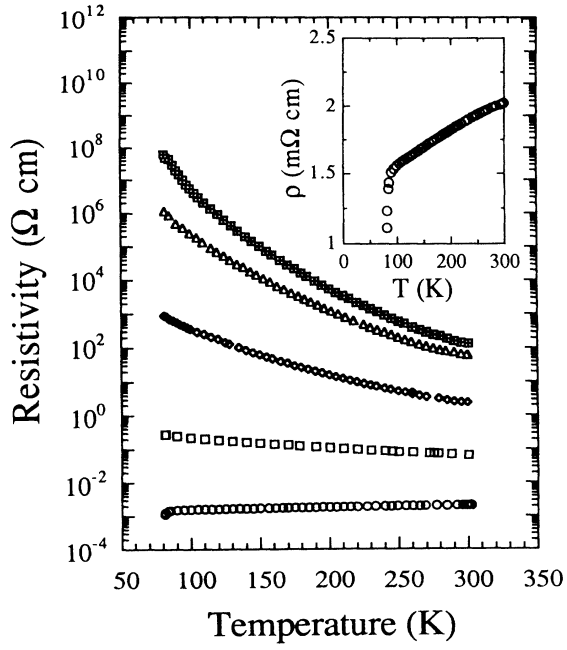

FIG. 6. Dark resistivity $\rho(T)$ of a DyBa$_2$Cu$_3$O$_{7-\delta}$ thin film as a function of temperature for a number of oxygen concentrations spanning the full range from the metallic and superconducting phase to the insulating antiferromagnetic phase. The different oxygen concentrations were obtained by aging the film at room temperature between the successive measurements of $\rho(T)$. In inset, $\rho(T)$ of the fresh DyBa$_2$Cu$_3$O$_{7-\delta}$ sample with $\delta\approx0$ (lowest-resistivity curve) is plotted on a linear scale.

In our studies of the DyBa$_2$Cu$_3$O$_{7-\delta}$ ultrathin epitaxial films, we found that after photoexcitation experiments at each low temperature (about 3–4 h of illumination or approximately 40 000 pulses with $I_L\approx10^{15}$–10^{16} photons/cm^2), the dark resistivity at that temperature decreased. This effect is shown in Fig. 7, where the dark resistivity is plotted for several different δ; in each case the sample was illuminated at $T\approx80$ K, and then the resistivity measurement was continued to lower temperatures (note the discontinuity in the data in each curve in Fig. 7). The higher the resistivity of the sample, the larger the decrease; more than one-order-of-magnitude decrease was observed in samples with resistivity of 10^8 Ω cm at 80 K, whereas only a 30% decrease was observed in samples with resistivity of 5×10^{-1} Ω cm at 80 K. This effect, we believe, is similar to that reported by Kirilyuk and co-workers[5,6] and confirms that long-time photoillumination can reduce the dark resistivity in thin films.

By comparing the data in Fig. 6 with the resistivity and activation energy from single crystals of YBa$_2$Cu$_3$O$_{7-\delta}$ with different δ, we estimate that the lowest-resistivity curve (in Fig. 6 and in the inset of Fig. 6) corresponds to $\delta\approx0$–0.2, while the highest-resistivity curve in Fig. 6 corresponds to $\delta\approx0.7$. The results illustrate that aging

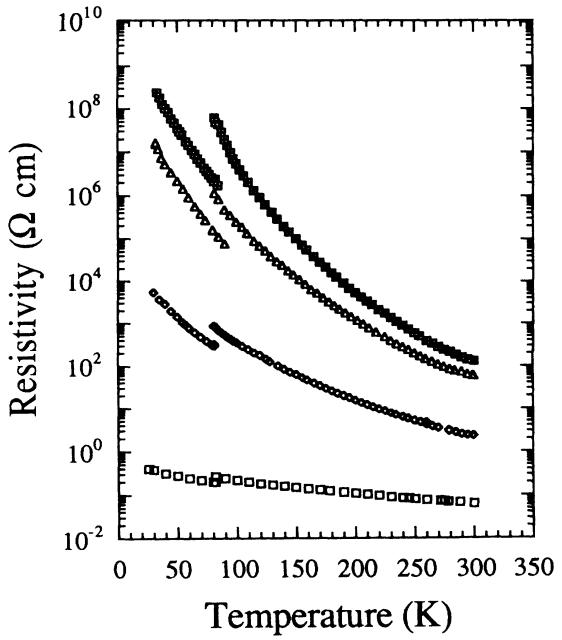

FIG. 7. Effect of long-term photoexcitation on the dark resistivity in a DyBa$_2$Cu$_3$O$_{7-\delta}$ film.

the thin films in dry air or vacuum is an effective method to obtain samples which are nearly ideal for photoinduced-conductivity studies with various oxygen concentrations.

In Fig. 8 we plot the results of transient photoinduced-conductivity measurements on an ultrathin film of $DyBa_2Cu_3O_{7-\delta}$ for two different oxygen contents with $\delta \approx 0.6$–0.7. Although there are data points for only a few temperatures, the transient photoinduced changes in resistivity are essentially identical to those shown in Fig. 3 for $YBa_2Cu_3O_{6.3}$. At high levels of excitation, the photoinduced resistivity of an ultrathin $DyBa_2Cu_3O_{6.3}$ film shows the three important features observed in the single crystals of $YBa_2Cu_3O_{6.3}$: a decrease in E_a of the photoinduced resistivity with increasing I_L, a superlinear dependence of the transient photoconductance on I_L, and a time delay in the growth of the peak photoconductance.

Direct comparison between the dark-conductivity data at different δ values (as shown in the Fig. 6) and the photoexcitation data at different light intensities at fixed δ [as shown in Figs. 8(a) and 8(b)] in the same film brings out another important feature. For a specific magnitude of the resistivity, the resistivities show similar temperature dependence, and they extrapolate to the same high-temperature value, no matter which method was used to bring the resistivity to that magnitude, i.e., by oxygen doping as shown in Fig. 6 or by photodoping as shown in Fig. 8.

These similarities indicate that the carrier density plays a dominant role in both the mechanism of charge transport and the M-I transition in the $MBa_2Cu_3O_{7-\delta}$ materials.

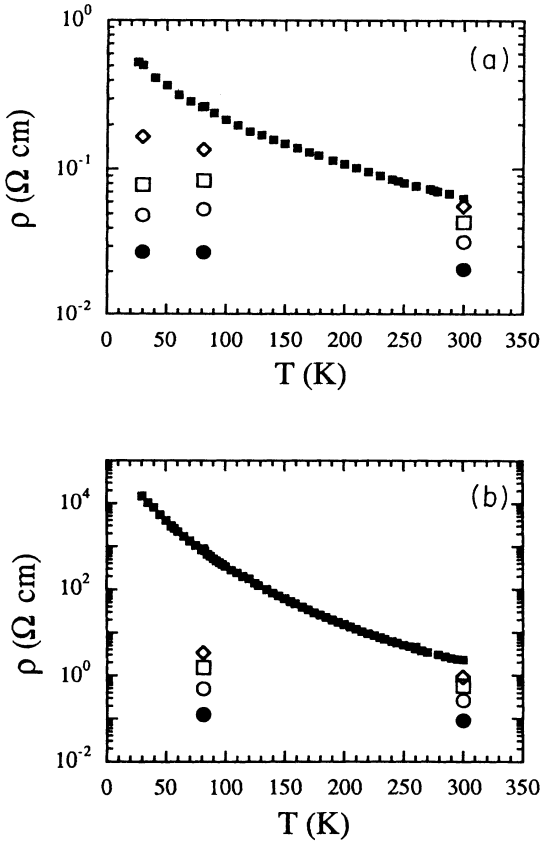

FIG. 8. Transient photoinduced resistivity in a 40-Å film of $DyBa_2Cu_3O_{7-\delta}$ for two different δ values. (a) $E_a \approx 23$ meV, $\delta \approx 0.6$: $I_L = 2.1\times10^{16}$ photons/cm^2 (●), $I_L = 7.2\times10^{15}$ photons/cm^2 (○), $I_L = 2.1\times10^{15}$ photons/cm^2 (□), and $I_L = 1\times10^{14}$ photons/cm^2 (◇). (b) $E_a \approx 108$ meV, $0.6 < \delta < 0.7$: $I_L = 2.1\times10^{16}$ photons/cm^2 (●), $I_L = 6.9\times10^{15}$ photons/cm^2 (○), $I_L = 2.1\times10^{15}$ photons/cm^2 (□), and $I_L = 1\times10^{15}$ photons/cm^2 (◇).

IV. "PHOTODOPING" TO THE METAL-INSULATOR TRANSITION

The phase diagram of $YBa_2Cu_3O_{7-\delta}$ $(0 \le \delta \le 1)$ has been studied thoroughly.[19] For large δ, $YBa_2Cu_3O_{7-\delta}$ is an antiferromagnetic insulator; increasing oxygen concentration introduced carriers onto the CuO_2 planes and results in the transition from the antiferromagnetic insulating phase to the metallic and superconducting phase. The changes in resistivity which occur during this evolution from insulator to metal (and superconductor) have been followed in detail in a continuous set of resistivity measurements of ultrathin films of $DyBa_2Cu_3O_{7-\delta}$ (as shown in Fig. 6).

Chemical doping (or substitution) of antiferromagnetic insulators has been used for many years to study the transition to the metallic state in highly correlated systems. An example which is closely related with high-temperature superconductors is $La_{1-x}Sr_xVO_3$.[20] The parent compound, $LaVO_3$, is an antiferromagnetic insulator which is made metallic by chemical doping with strontium. Disorder is introduced as a result of the random distributions of the La^{3+} and Sr^{2+} ions in the crystal. The results show that the disorder is sufficient to localize the electronic wave functions at Fermi level in the vanadium $3d$ band when $x < 0.2$. The experimental situation in $La_{2-x}Sr_xCuO_4$ is quite similar to that in the lanthanum-strotium vanadates, except that the vanadates do not become superconducting at low temperatures.[21] The changes in electronic transport in $MBa_2Cu_3O_{7-\delta}$ at different oxygen levels are comparable to those observed in $La_{1-x}Sr_xVO_3$ and $La_{2-x}Sr_xCuO_4$ as a function of the Sr content; in all cases the density of holes is changed by means of controlled changes in the chemical composition.

All of these systems show behavior characteristic of a metal-insulator transition which can be understood in the context of the Anderson theory[22] of disorder-induced localization of electronic states in the band tails, similar to that studied, for example, in doped semiconductors.[23] The disorder from mixed-valence substitution or partial oxygenation leads to the localization of the electronic states and, in turn, to the formation of a mobility edge at an energy E_c; hole states at energies $E > E_c$ are localized and hole states for $E < E_c$ are delocalized (extended). This situation is sometimes called weak localization. A metal-insulator transition occurs when the Fermi energy is moved through the mobility edge as a result of changing the carrier density by chemical doping or by photoexcitation ("photodoping").

A characteristic of disorder-induced localization as the origin of the M-I transition is the existence of a minimum metallic conductivity,[23] which can be deduced from the standard expression for the conductivity, $\sigma = ne^2\tau/m$ in the Ioffe-Regel limit[24] (the so-called dirty limit), where the mean free path is so small that it approaches the de Broglie wavelength of the electrons. For the anisotropic layered HTSC materials, a two-dimensional (2D) model is appropriate, and the minimum metallic conductivity is universal,[23,25]

$$\Sigma_{\min} \approx e^2/h \ , \tag{3}$$

where $e^2/h = 3.9\times10^{-5}\ \Omega^{-1}$. In the strict 2D limit, one can expect the measured sheet conductivity $\Sigma_{\min}$ to be related with the bulk conductivity $\sigma_{\min}$, as $\Sigma_{\min} = \sigma_{\min} c$, where c is the spacing between successive pairs of CuO_2 planes, which is equal to Å. In the "insulating" regime where $\sigma < \sigma_{\min}$, the conductivity becomes activated by thermal excitation from the Fermi energy E_F to the mobility edge E_c,

$$\sigma(T) = \sigma_{\min} \exp(-|E_c - E_F|/k_B T) \ , \tag{4}$$

in agreement with Eq. (1), where $|E_c - E_F|$ denotes $E_c > E_F$ for electrons and $E_c < E_F$ for holes. At lower temperatures variable-range hopping of carriers between the localized states near E_F becomes the dominant mechanism.

The effects of chemical doping on the conductivity of $DyBa_2Cu_3O_{7-\delta}$ and $YBa_2Cu_3O_{7-\delta}$ are consistent with the predictions of the localization theory.

(i) As inferred from the dark-conductivity data in Fig. 6 and the results presented in Ref. 14, $\sigma_{\min} \approx 35$ S/cm, which is obtained by using the nominal thickness of 40 Å. This value corresponds to a sheet conductivity of $\Sigma \approx (0.1-0.2)e^2/h$.

(ii) The resistivities naturally separate into two categories: When $\rho < 1/\sigma_{\min}$, the material is metallic and/or superconducting, and $\rho(T)$ in the normal state extrapolates to a finite (metallic) value as $T \to 0$; when $\rho > 1/\sigma_{\min}$, the material shows thermally activated behavior, and $\rho(T) \to \infty$ as $T \to 0$.

(iii) The comparison of the photoconductive response[3,26] and frequency-dependent conductivity (or absorption[18]) of $YBa_2Cu_3O_{6.3}$ implies localization of the low-energy states. Although there is strong absorption at energies throughout the midinfrared portion of the spectrum, this absorption does not lead to mobile carriers.[3,26]

Precisely the same features, indicating a M-I transition as the Fermi level is moved through the mobility edge, are observed as a result of the *photoinduced* carriers as shown in Figs. 3 and 4 for $YBa_2Cu_3O_{6.3}$ and in Fig. 8 for $DyBa_2Cu_3O_{7-\delta}$. From the activation energy of the dark conductivity [Eq. (4)], we conclude that E_F of the holes lies above E_c by about 0.2 eV in $YBa_2Cu_3O_{6.3}$ and by about 0.03 eV for $YBa_2Cu_3O_{6.4}$. Photodoping increases the hole density in a transient manner and shifts the Fermi level toward the mobility edge as indicated by the E_a approaching 0 at high light intensities (as shown in Fig. 5). The extrapolation to $1/T \to 0$ determines the sheet conductivity to be about $5\times10^{-6}\ \Omega^{-1}$ [$\approx(0.1-0.2)e^2/h$].

The smaller observed value of the minimum metallic conductivity per layer [about 0.2 of the value estimated in Eq. (3)] might be due to error in the absolute value arising from the experimental configuration; i.e., since the Auston switch is a two-probe configuration and the photoconductivity is calculated by treating the photocurrent distributed uniformly within the optical depth (300 Å), such precision is beyond the accuracy of the transient photoconductivity experiment. In particular, we are certainly underestimating the true sheet conductance; because the electrodes are contacted to the sample in front-surface geometry and because of the higher resistance in the c direction, the deeper CuO_2 planes can be expected to contribute less to the photocurrent.

The $DyBa_2Cu_3O_{6.3}$ data of Fig. 6 are replotted on a semilogarithmic scale as ρ vs $1/T$ in Fig. 9. As shown, extrapolation to $1/T \to 0$ yields $\rho_0 \approx 3\times10^{-2}\ \Omega$ cm for $DyBa_2Cu_3O_{7-\delta}$. In this case the accuracy in the volume resistivity is also limited by the uncertainty in the film thickness (the 40-Å nominal value). The sheet conductivity obtained from ρ_0/c is about 5×10^{-6} S/sheet [$\approx(0.1-0.2)e^2/h$].

The consistent agreement between dark-conductivity data obtained with different oxygen concentrations, the photoconductivity obtained with different pump light intensities at a given oxygen concentration, and the predictions of 2D localization theory implies that disorder-induced localization of the carriers is the most important reason for the M-I transition. Obviously, this does not imply that correlation effects arising from the electron-electron Coulomb interaction are unimportant in these systems. As Mott pointed out,[21,27] the repulsive electron-electron interaction results in a demarcation energy E_F', separating singly occupied from doubly occu-

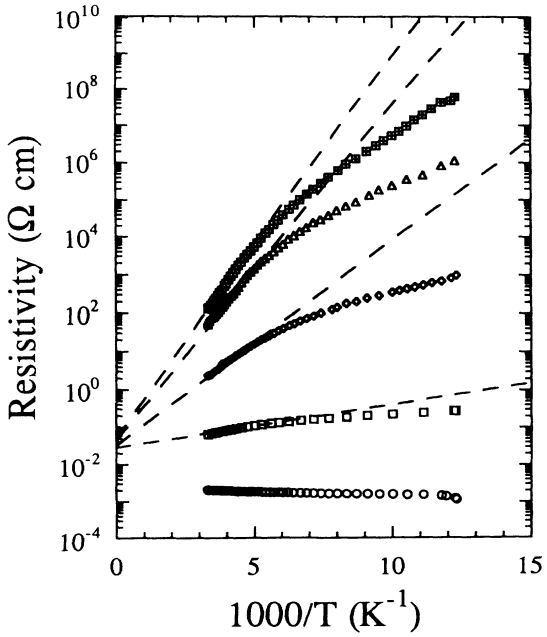

FIG. 9. Dark resistivity $\rho(T)$ of $DyBa_2Cu_3O_{7-\delta}$ (from Fig. 6) plotted vs $1000/T$; the dashed lines are guides to the eye.

pied states, the separation corresponding to the Hubbard intrastate interaction for one of the Anderson localized states. As localization becomes stronger and stronger, E_F' will sink until all states are singly occupied, with important consequences. For example, relatively strong electron-electron interactions account for the antiferromagnetic ordering in the Fermi-glass phase and imply that above the Néel temperature the moments of the singly occupied states fluctuate between random directions. Nevertheless, the data presented and analyzed in this section indicate that the electron-electron interaction has a secondary effect on the *M-I* transition.

It is relevant to quantitatively compare the light intensity required to achieve the *M-I* transition through photoexcitation with the oxygen-doping level required for chemically inducing the *M-I* transition. For example, it is known that the *M-I* transition in $YBa_2Cu_3O_{7-\delta}$ occurs near $\delta \approx 0.55-0.6$.[19] For single crystals of $YBa_2Cu_3O_{6.3}$, about 15% more oxygen per cell [approximately $(1.0-1.5)\times 10^{21}$ atoms/cm^3] is needed to switch the system from the semiconducting phase to the metallic and superconducting phases. In the transient photoconductivity experiment, the critical photon density (to reach the superlinear regime where the activation energy turns to zero) is about $(5-7)\times 10^{15}$ photons/cm^2, corresponding to 2×10^{21} photons/cm^3 within the optical-absorption depth.[18] Assuming that the quantum efficiency is unity at the time of photocurrent peak, then the density of the photoinduced charge carriers required to reach the *M-I* transition is of the same magnitude as the density of the extra dopants (oxygen atoms) required to induce the *M-I* transition. Because of phase separation of the photogenerated carriers (see following section), the actual quantum efficiency could be considerably smaller than unity at the peak of the photoinduced conductivity.

V. MINIMUM IN $\rho_{ph}(T)$: PHASE SEPARATION AND PHOTOINDUCED HIGH-T_c SUPERCONDUCTIVITY

We have shown that by transient "photodoping," one can induce sufficient density of carriers to $YBa_2Cu_3O_{6.3}$ to shift the Fermi level to the mobility edge and to take the material to the borderline of metallic behavior. The obvious question is whether or not such a transient borderline metal can condense to the superconducting phase.

The observation of the minimum in $\rho_{ph}(T)$ at the highest excitation levels (see Fig. 3) is suggestive of the onset of photoinduced transient superconductivity. Curves similar to that in Fig. 3 were seen frequently during the period following the discovery of high -temperature superconductivity in resistivity measurements on samples with multiphase composition. Such behavior is indicative of phase separation with disconnected metallic-superconducting regions separated by insulating regions: the decrease in $\rho(T)$ near 100 K is due to the onset of superconductivity, and the increase in $\rho(T)$ at lower temperatures is due to the "series resistance" of the insulating regions. Similar phenomena are observed in granular superconducting films which exhibit local superconductivity with tunneling between grains.[8,9] It is well known that, in this type of material, the transport behavior depends strongly on the cluster size. The resistivity of the sample decreases rapidly below T_c, but does not go to zero, increasing again at low temperature under circumstances where the clusters are not macroscopically connected (below the percolation threshold). This phenomenon has been called "local superconductivity."[8] An important similarity between the phenomenon of local superconductivity and the $\rho_{ph}(T)$ data in$YBa_2Cu_3O_{6.3}$ as those shown in Fig. 3 is that T_c does not change with the cluster size or, in the case of photoexcitation, with photon density. The similarities in both the magnitude and shape of $\rho(T)$ imply that the photoinduced charge carriers phase separate and become inhomogeneously distributed after photogeneration.

Theoretical studies of the two-dimensional antiferromagnet[28–30] have shown that dilute holes are unstable against phase separation into a hole-rich phase and a pure antiferromagnetic insulating phase; no region in the zero-temperature phase diagram was found in which a dilute gas of holes is stable. These theoretical results suggest that phase separation might be an intrinsic feature in the $MBa_2Cu_3O_{7-\delta}$ family, whether the carriers are injected through changes in the oxygen level or through photodoping.

It is also well known[23(a)] that in materials similar to the HTSC oxides, chemical phase separation is a common phenomenon; it is typically necessary to thermally anneal specimens at high temperatures to obtain a more homogeneous phase. At the relatively high temperatures at which the materials are grown, the increased entropy associated with the dilute holes may partially overcome the tendency for phase separation, leading to a somewhat more uniform oxygen content throughout the $YBa_2Cu_3O_{7-\delta}$ series. Since, however, the photoexcitation is carried out at lower temperatures, entropic contributions to the free energy are less important, and more complete phase separation would be expected.

Because of the phase separation, the transport will be dominated by the insulating regions until the metallic droplets become connected above the percolation transition. Thus, in the $YBa_2Cu_3O_{6.3}$ experiments, the insulating regions between metallic droplets would be expected to have conductivity intermediate between that of $\delta=0.7$ and the δ corresponding to σ_{min} (near 0.55–0.6). Metallic particles encapsulated in an insulator have been investigated for many years.[31] If the particles are small and not in direct contact, an activation energy (associated with the capacitance energy for adding one extra charge to a small particle) is necessary for the transport of charge from one particle to another. This may also contribute to the residual activation energy in the photoinduced-conductivity experiments at light intensities above 10^{15} photons/cm^2 (as shown in Figs. 4 and 5).

There is supporting evidence indicating phase separation of the photogenerated carriers.

(i) the onset of superconductivity (as indicated by the onset of the resistivity decrease in Fig. 3) is approximately that of the highest doped material, $YBa_2Cu_3O_7$—i.e., the droplets appear to be well into the metallic regime.

(ii) During photoexcitation, the absorbed photons

create electron-hole pairs in the CuO_2 planes. The electrons will be quickly trapped at oxygen vacancies on adjacent partially oxidized CuO chains and would tend to enhance locally the orthorhombic distortion, as observed in the photoinduced-absorption experiments.[32]

(iii) Although the holes are initially photogenerated uniformly within the optical-absorption depth, hole mobility is inhibited by the antiferromagnetic phase-separated droplets (as is shown in the calculations with t-J-U model[28–30]) results in locally hole-rich regions with relatively high mobility, causing a diffusion-limited increase in $\mu(t)$ and, thereby, the photoconductance [see Eq. (2)]. The competition between this effect and charge-carrier recombination results in the delay of the *peak* photocurrent evident in the data of Fig. 2. As the pump-light intensity increases, the hole density in the resulting hole-rich regions is sufficient to shift the Fermi level through the mobility edge, to locally convert these regions into the metallic and superconducting phase, and to decrease the total resistivity of the (partially) phase-separated system.

(iv) The frequencies of the infrared-active vibrational (IRAV) modes observed in photoinduced absorption do not correlate with the Raman modes of the insulating phase, but they do correlate with the Raman modes of the metallic phase.[32,33] This is true even in $Tl_2Ba_2Ca_{1-x}Gd_xCu_2O_8$ where the semiconductor ($x=0.02$) and metal ($x=0$) have the same structure.[32,33] These results imply that photodoping leads to metallic screening and associated shifts in the phonon frequencies characteristic of the metallic phase, consistent with droplet formation. Isolated holes would not give a IRAV mode correlated with the metallic phase, especially when the crystal structure is the same in both cases. Moreover, in spite of the relatively large shifts ($\Delta\omega \sim 50$–$100\ cm^{-1}$), the IRAV modes are narrow and well defined, indicating a long range for the metallic phase and therefore consistent with phase separation; otherwise, a broad featureless band covering the entire $\Delta\omega$ would be observed.

Although we do not have any direct experimental information on the length scale for the phase separation, the size of the droplets must be at least comparable to or larger than the pairing coherence length [$\zeta \approx 15$ Å (Ref. 34)] in the high-T_c materials.

VI. EXPERIMENTS ON $YBa_2Cu_3O_{6.4}$: EVIDENCE OF METASTABILITY AT HIGH LEVELS OF PHOTOEXCITATION

Figure 10 shows a series of transient decay curves following different levels of photoexcitation for a sample with oxygen content even closer to the M-I transition, $YBa_2Cu_3O_{6.4}$; the data were taken at 35 K. Since, for this sample, $E_a \approx 0.03$ eV, a full set of experiments, for example, at temperatures $T > 50$ K, were not possible because of the low resistivity. At $I_L = 4.5\times10^{14}$ photons/cm^2, the magnitude of the transient photoconductivity is more than an order of magnitude below the value corresponding to the universal sheet conductance ($\sigma_{min} \approx 20$ S/cm; see Fig. 4), and the time decay of the conductivity follows a power law ($\approx t^{-\alpha}$). With increasing light intensity, the

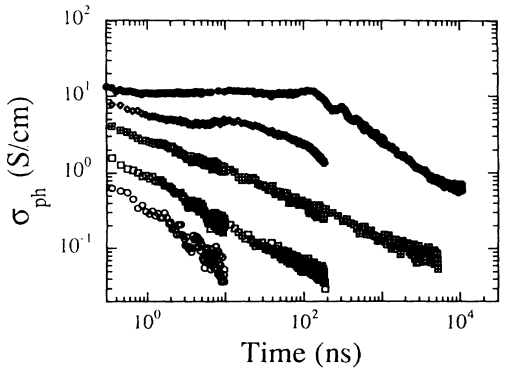

FIG. 10. Decay of the photoinduced conductivity for $YBa_2Cu_3O_{6.4}$ at 35 K: $I_L = 4.5\times10^{14}$ photons/cm^2 (○), $I_L = 8.6\times10^{14}$ photons/cm^2 (□), $I_L = 2.1\times10^{15}$ photons/cm^2 (⊞), $I_L = 4.4\times10^{15}$ photons/cm^2 (◇), and $I_L = 1\times10^{16}$ photons/cm^2 (●).

magnitude of σ_{ph} approaches σ_{min}, and the exponent of the power law decreases significantly. Finally, when the pump-light intensity is strong enough to photogenerate the metallic state ($\sigma_{ph} \approx \sigma_{min}$), the photoconductivity persists at $\sigma_{ph} \approx \sigma_{min}$ to times in excess of 100 ns, corresponding to enhancement of the lifetime by approximately three orders of magnitude (see Fig. 10). Similar results have been obtained for $La_2CuO_{4+\delta}$.[35]

The time decay of the photoinduced conductivity is determined by Eq. (2), where both $n_c(t)$ and $\mu(t)$ are time dependent; $n_c(t) \rightarrow 0$ as the carriers recombine and the system approaches the ground state; $\mu(t) \rightarrow 0$ as a result of the trapping of carriers in localized states.

The power-law decay of the transient photoinduced conductivity at low excitation levels is consistent with dispersive transport of the carriers, as expected in disordered systems[35] where the Fermi level lies between E_F and E_c in the range of energies for which the electronic states are localized. Since the localized states act as traps, charge transport is realized via a sequence of multiple-trapping and release steps among localized states in the presence of an applied electric field.[23] Because of the disorder, the transfer time is a random variable. Thus the accumulated sequence of these transfer events in the motion of a charge carrier can be viewed as a continuous-time random walk, and the resulting photocurrent follows a power-law time dependence $t^{-(1-\beta)}$, where the exponent β is related with the decay power α,[36]

$$\alpha = 1-\beta\ , \tag{5}$$

and β can be expressed as

$$\beta = T/T_0\ . \tag{6}$$

In the simplified model of an exponential distribution of the trap (localized-state) density, T_0 specifies the energy range over which the localized trap states can be filled.[36] For example, in the insulating phase of HTSC oxides, $k_B T_0$ corresponds to the energy between the Fermi level

and the mobility edge, $|E_F - E_c|$ (the activation energy in resistivity measurements) so that

$$\beta \approx k_B T / E_a \ . \tag{7}$$

The data at low excitation levels in Fig. 10 are consistent with dispersive transport. Since the thermal activation energy in the dark resistivity is about 33 meV in this sample (the Fermi level of the holes lies above the mobility edge by about 33 meV), at temperatures near 300 K ($k_B T = 26$ meV), the density of thermally activated charge carriers at the mobility edge is so large that photoinduced-conductivity measurements become essentially impossible (the density of photo-excitations is less than the density of thermal excitations, and the resistivity is too low to support bias voltage without damaging the sample). At 35 K (corresponding to 3 meV, so that $\beta \approx k_B T / E_a \approx 0.1$), the density of thermally excited carriers is negligible, and photoinduced conductivity can be observed as shown in Fig. 10. The exponent in the time decay of $\sigma_{\rm ph}$ at the lowest light intensity is $\alpha \approx 0.9$, which is consistent with Eqs. (5)–(7). Within this model, at a fixed temperature, a decrease in β on increasing the light intensity implies a shift in the Fermi level toward the mobility edge, indicating an approach to the M-I transition by photoexcitation, consistent with the fact that $\sigma_{\rm ph}$ approaches $\sigma_{\rm min}$.

At higher excitation levels, the photoinduced conductivity persists at $\sigma \approx \sigma_{\rm min}$ to times in excess of 100 ns. This remarkable persistence of the photoinduced conductivity at $\sigma \approx \sigma_{\rm min}$ suggests metastability in $n_c(t)$, consistent with the phase separation and the formation of metallic droplets.

VII. MAGNETIC-FIELD SUPPRESSION OF THE PHOTOINDUCED CONDUCTIVITY

Motivated by the interpretation of the minimum in $\rho_{\rm ph}(T)$ at high excitation levels as indicative of the onset of the photoinduced transient superconductivity, we have carried out a series of transient photoinduced-conductivity measurements in the presence of a modest external magnetic field (≤ 0.5 T). In these experiments the geometry is chosen such that the magnetic-field direction is parallel to the applied electric field so that effects due to the Lorentz force (e.g., both the Hall effect and magnetoresistivity) would be eliminated.

In Fig. 11(a) we compare the peak photoconductance ($G_{\rm ph}$) as a function of the excitation intensity for $B = 0$ and 0.5 T for $YBa_2Cu_3O_{6.3}$ at 60 K. The data were taken with field on and off, alternately, at fixed temperature. The differential photoconductance $\Delta G_{\rm ph}(B) = [G_{\rm ph}(B = 0) - G_{\rm ph}(B = 0.5\ {\rm T})]$, is plotted versus I_L in Fig. 11(b). A magnetic-field dependence is observed at excitation levels

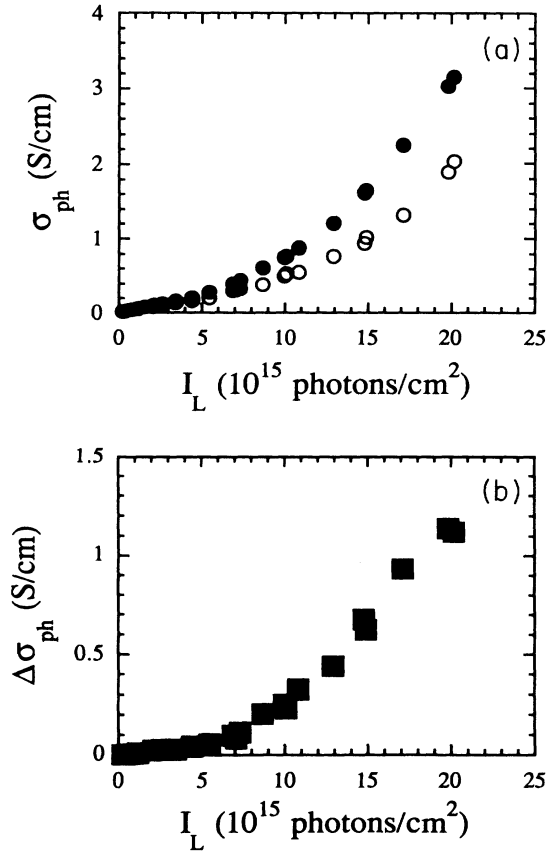

FIG. 11. (a) Peak photoconductivity $\sigma_{\rm ph}$ of $YBa_2Cu_3O_{6.3}$ ($E_a \approx 0.22$ eV) plotted as a function of excitation intensity (I_L) for $B = 0$ (●) and $B = 0.5$ T (○) at 60 K; (b) $\Delta\sigma_{\rm ph} = [\sigma_{\rm ph}(B = 0) - \sigma_{\rm ph}(B = 0.5T)]$ is plotted vs I_L.

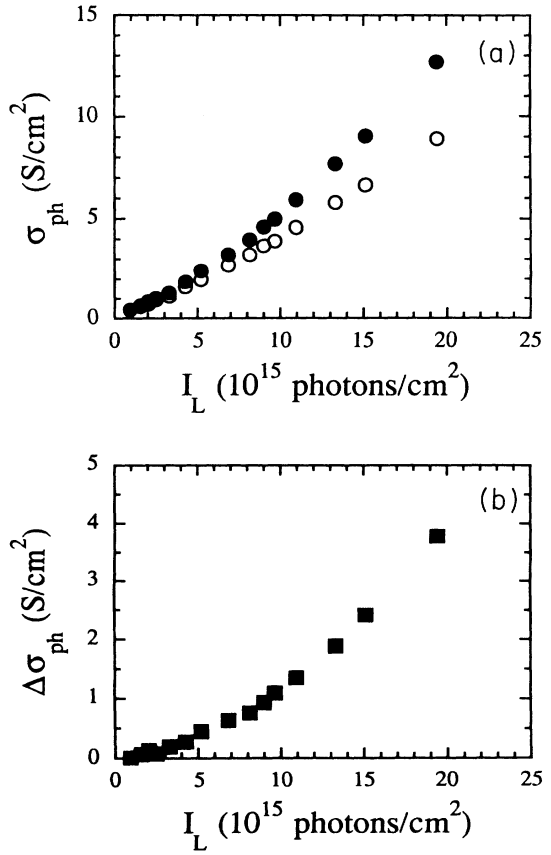

FIG. 12. (a) Peak photoconductivity $\sigma_{\rm ph}$ in a film of $DyBa_2Cu_3O_{7-\delta}$ with δ near 0.6 [as in Fig. 8(a)] plotted as a function of excitation intensity (I_L) at 80 K for $B = 0$ (●) and $B = 0.5$ T (○); (b) $\sigma_{\rm ph} = [\sigma_{\rm ph}(B = 0) - \sigma_{\rm ph}(B = 0.5T)]$ vs I_L.

above a critical I_L, which is coincident with the onset of the superlinear dependence, coincident with the onset of metallic behavior, and coincident with the onset of the minimum in $\rho(T)$. In Fig. 12 we show similar results obtained from a $DyBa_2Cu_3O_{7-\delta}$ thin film with δ near 0.6. Figure 13(a) shows the dependence of $\rho_{ph}(B)$ for $YBa_2Cu_3O_{6.3}$, $\Delta\rho_{ph}/\rho_{ph} \sim |\Delta G_{ph}/G_{ph}| \sim B^{1/2}$ as shown in Fig. 13(b). We checked carefully for magnetic-field dependence of the dark (direct-current) resistivity; none could be detected ($\Delta G/G < 10^{-4}$).

Figure 14 plots the time evolution of the transient photoconductivity of $YBa_2Cu_3O_{6.3}$ for $B=0$ and 0.5 T; the magnetic field suppresses the transient transient photoinduced conductivity. The data show the following: (a) The magnetic field suppresses the superlinear contribution to the transient photoinduced conductivity at $I_L \geq 5\times10^{15}$ photons/cm^2; (b) the peaks of the *differential* photocurrents are time delayed with respect to the excitation laser pulses, implying that the time delay associated with the growth of carrier mobility is magnetic-field dependent (longer time delay at zero field). Comparison of the $B=0$ and 0.5 T profiles in Fig. 14 indicates that the time delay at zero field is greater than at 0.5 T by approximately 200 ps. Although the measurement of the precise value of the change in time delay would benefit from higher-resolution measurements, the effect is real; higher-resolution measurements of the magnetic-field dependence in $YBa_2Cu_3O_{6.3}$ and $YBa_2Cu_3O_{6.4}$ are planned for future experiments.

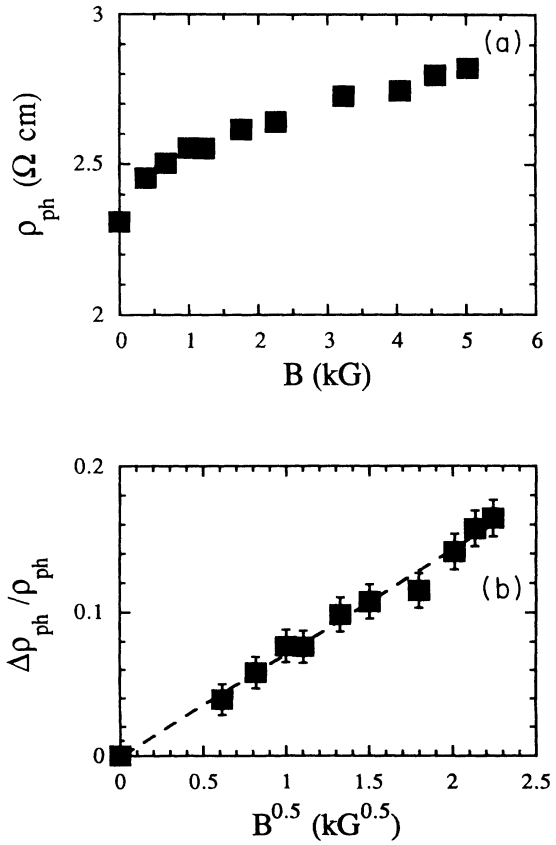

FIG. 13. (a) Photoinduced magnetoresistivity in $YBa_2Cu_3O_{6.3}$ ($E_a \approx 220$ meV) is plotted as a function of the longitudinal magnetic field at 60 K under light intensity of 1.5×10^{16} photons/cm^2. (b) Data in (a) are replotted as $\Delta\rho_{ph}/\rho_{ph}$ vs $B^{1/2}$.

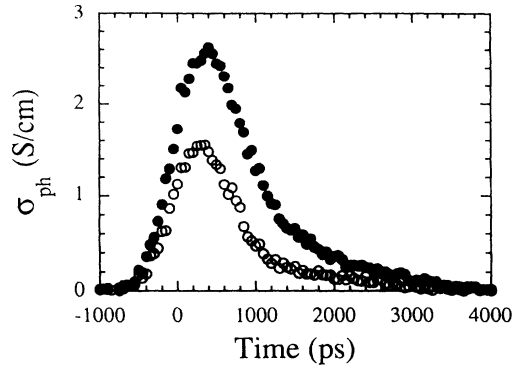

FIG. 14. Time evolution of the transient photoconductivity in $YBa_2Cu_3O_{6.3}$ ($E_a \approx 220$ meV) for $B=0$ (●) and $B=0.5$ T (○) at 80 K with $I_L = 1.5\times10^{16}$ photons/cm^2. The excitation source was the N_2 laser; the instrumental resolution is similar to that in Fig. 1(a).

We have interpreted the time delay in the peak photoconductance in $YBa_2Cu_3O_{6.3}$ as resulting from the competition between the diffusion-limited increase in $\mu(t)$ and the decrease in $n_c(t)$ through charge-carrier recombination. Thus the increased time delay at high I_L seen in the results obtained in a magnetic field indicates a somewhat longer recombination time and/or metastability in the phase-separated state, consistent with the data in Fig. 10. In Fig. 15 the time evolution of the transient photoconductivity in $YBa_2Cu_3O_{6.3}$ is shown at two light intensities; the data were taken at 80 K. A decrease in the time delay is observed upon decreasing the light intensity, similar to that observed (at high I_L) when the magnetic field is turned on.

It is tempting to associate the magnetic-field suppression with the onset of transient photoinduced superconductivity, for example, by magnetic-field suppression of Josephson coupling between superconducting droplets. We note, however, that the magnetic-field effect is ob-

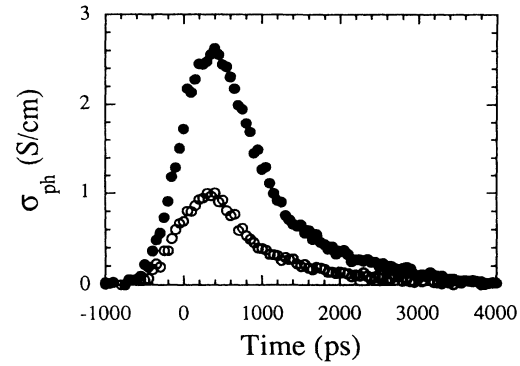

FIG. 15. Time evolution of the transient photoconductivity in $YBa_2Cu_3O_{6.3}$ ($E_a \approx 220$ meV) at two different light intensities at levels $\sim1\times10^{16}$ photons/cm^2 (○) and $\sim1.5\times10^{16}$ photons/cm^2 (●), both at 80 K.

served at all temperatures, even well above 100 K. Thus the magnetic-field suppression of the transient photoinduced conductivity may be a more general feature of the M-I phase boundary.

VIII. POTENTIAL ARTIFACTS: SAMPLE HEATING OR PHOTOGENERATED CARRIERS?

The most obvious potential artifact in photoexcitation experiments is resistance changes which result from surface heating (ΔT), caused by the light absorption, rather than genuine transient photoinduced conductivity. The importance of sample heating was carefully and thoroughly examined.

(i) To obtain the observed change in ρ from heating, ΔT would have to exceed the melting temperature (see Fig. 4). However, even after thousands of laser shots, there is no indication of surface damage.

(ii) The maximum (peak) temperature increase ΔT expected from laser heating occurs at a time $t_h \approx 0.5\tau$ with magnitude $\Delta T \sim N\tau^{1/2}$, where τ is the laser-pulse width and N is the number of photons deposited during the pulse.[16] In contrast, neither the magnitude of the peak photocurrent nor the time delay are dependent on the width of the excitation pulse, which has been varied from 30 to 600 ps (see Fig. 2).

(iii) The nonmonotonic T dependence (see Fig. 3) observed at high I_L is not consistent with heating.

(iv) Essentially identical features are observed for single crystals and 40-Å, films. Since the latter absorb only $\approx 10\%$ of I_L,[18] ΔT would be smaller than in the crystals by an order of magnitude. Thus one would expect a several-orders-of-magnitude reduction in the signal if it were caused by surface heating.

(v) The remarkable enhancement of the lifetime (Fig. 10) with $\sigma \approx \sigma_{\min}$ to times in excess of 100 ns is not consistent with heating.

(vi) The changes in the time profile of the photoinduced conductivity (Fig. 14) at high excitation levels (Fig. 12) for $B = 0.5$ T as compared with $B = 0$ are not consistent with heating.

We conclude, therefore, that *sample heating is not a serious factor in our transient photoinduced-conductivity experiments;* the photoresponse arises from photoexcited carriers and genuine photoconductivity.

IX. CONCLUSION

We have demonstrated *photodoping* of $YBa_2Cu_3O_{6.3}$ and $DyBa_2Cu_3O_{6.3}$ to borderline metallic-superconducting levels. Two specific signatures of the transient photoinduced transition to metallic behavior at light intensities greater than about 5×10^{15} photons/cm^2 were observed: The activation energy of $\sigma_{ph}(T)$ decreases as a function of the light intensity and approaches zero for $I_L \approx 5\times10^{15}$ photons/cm^2; and a minimum appears below 100 K in the temperature dependence of the photoresistivity, $\rho_{ph}(T) = 1/\sigma_{ph}(T)$.

The minimum in $\rho_{ph}(T)$ is reminiscent of the onset of superconductivity in inhomogeneous mixed-phase HTSC samples and similar to the "local superconductivity" found in granular metallic films. Such behavior is indicative of phase separation and metallic-droplet formation subsequent to photoexcitation with disconnected superconducting regions separated by insulating regions: The decrease in $\rho_{ph}(T)$ near 100 K is due to the onset of superconductivity, and the increase in $\rho_{ph}(T)$ at lower temperatures is due to the "series resistance" of the insulating regions.

The data are consistent with disorder-induced localization as the origin of the metal-insulator transition. Analysis of the temperature dependence of the dark conductivity of $DyBa_2Cu_3O_{7-\delta}$ for different δ and the temperature dependences of $YBa_2Cu_3O_{6.3}$ and $DyBa_2Cu_3O_{6.3}$ for different I_L yield minimum surface conductances which are consistent with $\Sigma_{\min} \approx e^2/h$, the value predicted for two dimensions where the minimum metallic conductivity is universal. The data separate into two categories: when $\Sigma > \Sigma_{\min}$, the material is metallic, and when $\Sigma < \Sigma_{\min}$, the material shows thermally activated behavior.

A longitudinal magnetic field (≤ 0.5 T) suppresses the superlinear contribution to the transient photoinduced conductivity at $I_L \geq 5\times10^{15}$ photons/cm^2. Moreover, the time profiles of the transient photoconductance in $YBa_2Cu_3O_{6.3}$ demonstrate that the time delay associated with the growth of carrier mobility is magnetic-field dependent with a longer time delay at $B = 0$ than at $B = 0.5$ T by about 250 ps. We have interpreted the time delay in the peak photoconductance as resulting from the competition between the diffusion-limited increase in $\mu(t)$ due to phase separation and the decrease in $n_c(t)$ through charge-carrier recombination. Thus the increased time delay at high I_L suggests a somewhat longer recombination time or metastability in the phase-separated state at high I_L. This increase in the photoexcitation lifetime is suppressed by the magnetic field. Metastability of the photoexcited metallic phase is observed for $YBa_2Cu_3O_{6.4}$ where the lifetime of the photoexcited system is enhanced by three orders of magnitude following photoexcitation to high levels.

In conclusion, the experimental results summarized in Figs. 1–15 have the following implications: (1) The photoexcitations phase separate into metallic droplets. (2) The metallic regions go superconducting below T_c of the heavily doped material. (3) The photogenerated metallic state is metastable; the lifetime is enhanced by several orders of magnitude in samples with δ near the M-I transition. (4) The M-I transition is caused principally by disorder-induced localization arising from the random distribution of oxygen in the O(1) sites. Perhaps of equal importance is the sheer magnitude of the observed phenomena. The photoinduced-conductivity changes span 10–15 orders of magnitude or even greater, depending on the temperature, and the lifetime of the photoinduced conductivity is enhanced by more than three orders of magnitude at high levels of excitation.

The data have further implications, for they are directly relevant to the primary focus of the field, the mechanism of high-temperature superconductivity. Theoretical studies of the two-dimensional antiferromagnet conclude

that dilute holes are unstable against phase separation into a hole-rich phase and a pure antiferromagnetic insulating phase.[28–30] Since no region in the phase diagram was found in which a dilute gas of holes is stable, phase separation might be intrinsic in $YBa_2Cu_3O_{7-\delta}$ whether carriers are injected through changes in δ or through photodoping. Moreover, Emery and Kivelson[29] have argued that dynamic phase separation (fluctuations in the carrier density at intermediate-length scales) can lead to pairing.

Photodoping is indeed an attractive alternative method to vary the concentration of charge carriers. By increasing n_c at fixed δ, we have been able to move the Fermi level through the mobility edge and thereby investigate the origin of the metal-insulator transition without simultaneously changing the degree of disorder. By using pulsed-laser excitation, we have succeeded in increasing n_c to metallic levels in a transient manner with subnanosecond resolution. The measurements involve thousands of pulses at 10^{16} photons/cm^2 without significant sample degradation during a measurement, implying that one can switch the material between the insulating phase and metallic or superconducting phase effectively. Therefore, in addition to their theoretical significance in the context of phase separation and the photoinduced metallic or superconducting state, the results imply a potential for applications (photoinduced superconducting switch). The extension of these studies to shorter times (by using shorter pulses and improved temporal resolution) and to higher levels of excitation promises to be particularly interesting.

ACKNOWLEDGMENTS

We thank Dr. S. D. Phillips, Dr. D. Mihailvoc, and Dr. C. M. Foster for valuable discussions on photoexcitation phenomena, Karl Voss and Dr. D. Moses for a number of useful comments and suggestions, and Professor J. R. Schrieffer and Professor D. J. Scalapino for their stimulating comments on HTSC. The x-ray experiments in single crystals of $YBa_2Cu_3O_{6.3}$ were carried out by L. C. Chen. The photoinduced conductivity and related characterization measurements were carried out at UCSB and supported by a NSF SGER grant (No. DMR 91-02634) and by a UC (INCOR Grant No. LLNI-Incore 908A95). The ultrathin Dy-Ba-Cu-O films were prepared at Minnesota with partial support by the NFS/MGR program under Grant No. NSF/DMR-8908094, by the AFOSR under Grant No. AFOSR-87-0372, and by the Department of Administration of the State of Minnesota. The Y-Ba-Cu-O single-crystal samples were prepared at E. I. du Pont de Nemours and Co., Inc. (Central Research and Development Department).

[1]J. G. Bednorz and K. A. Müller, Z. Phys. B **64**, 198 (1986).

[2]For recent reviews, see, for examples, (a) *Physical Properties of High Temperature Superconductors,* edited by D. M. Ginsberg (World Scientific, Singapore, 1990), Vols. I and II; (b) *High Temperature Superconductivity,* Proceedings of Los Alamos Symposium, 1989, edited by K. S. Bedell, D. Coffey, D. E. Meltzer, D. Pines, and J. R. Schrieffer (Addison-Wesley, New York, 1990).

[3]G. Yu, A. J. Heeger, G. Stucky, N. Herron, and E. M. McCarron, Solid State Commun. **72**, 345 (1989).

[4]Tineke Thio, R. J. Birgeneau, A. Cassanho, and M. A. Kastner, Phys. Rev. B **42**, 10 800 (1990).

[5]A. I. Kirilyuk, N. M. Kreines, and V. I. Kudinov, Pis'ma Zh. Eksp. Teor. Fiz. **52**, 696 (1990) [JETP Lett. **52**, 49 (1990)].

[6]V. I. Kudinov, N. M. Kreines, A. I. Kirilyuk, R. Laiho, and E. Lahderanta, Phys. Lett. A **151**, 358 (1990).

[7]G. Yu, C. H. Lee, and A. J. Heeger, N. Herron, and E. M. McCarron, Phys. Rev. Lett. **67**, 2581 (1991).

[8]H. M. Jaeger, D. B. Haviland, B. G. Orr, and A. M. Goldman, Phys. Rev. B **40**, 182 (1989); D. B. Haviland, H. M. Jaeger, B. G. Orr, and A. M. Goldman, *ibid.* **40**, 719 (1989); D. B. Haviland, Y. Liu, T. Wang, and A. M. Goldman, Physica B **169**, 238 (1991).

[9]R. C. Dynes, J. P. Garno, and J. M. Rowell, Phys. Rev. Lett. **40**, 479 (1978).

[10]G. Yu, C. H. Lee, A. J. Heeger, N. Herron, and E. M. McCarron (unpublished).

[11]D. A. Auston, in *Picosecond Optoelectronic Devices,* edited by Chi H. Lee (Academic, New York, 1984), Chap. 4; M. V. Schneider, Bell Syst. Tech. J. **48**, 1421 (1960).

[12]B. R. Johnson, K. M. Beauchamp, T. Wang, J-X. Liu, K. A. McGreer, J-C. Wan, M. Tuominen, Y-J. Zhang, M. L. Mecartney, and A. M. Goldman, Appl. Phys. Lett. **56**, 1911 (1990).

[13](a) The x-ray experimental results indicated that the $YBa_2Cu_3O_{7-\delta}$ crystals used in our experiments were in single phase with tetragonal structure; the cell parameters were $a=b=3.8655$ Å and $c=11.757$ Å for the samples of $E_a\approx 0.20$ eV, which is determined to be $YBa_2Cu_3O_{6.3}$ according to the literature values; (b) J. M. Tarascon, P. Barboux, B. G. Bagley, L. H. Greene, W. R. McKinnon, and G. W. Hull, in *Chemistry of High-Temperature Superconductors,* edited by D. L. Nelson, M. S. Whittingham, and T. F. George (American Chemical Society, Washington, D.C., 1987), Chap. 10.

[14]T. Wang, K. M. Beauchamp, D. D. Berkley, B. R. Johnson, J-X. Liu, J. Zhang, and A. M. Goldman, Phys. Rev. B **43**, 8623 (1991).

[15]W. E. Pickett, Rev. Mod. Phys. **61**, 433 (1989); J. H. Weaver, H. M. Meyer III, T. J. Wagener, D. M. Hill, Y. Gao, D. Peterson, Z. Fisk, and A. J. Arko, Phys. Rev. B **38**, 4668 (1988); R. S. List *et al.* **38**, 11 966 (1988).

[16]J. H. Bechtel, J. Appl. Phys. **46**, 1585 (1975).

[17]S. G. Han, Z. V. Vardeny, K. S. Wong, and O. G. Symko, Phys. Rev. Lett. **65**, 2708 (1990); S. D. Brorson, A. Kazeroonian, D. W. Face, T. K. Cheng, G. L. Doll, M. S. Dresselhaus, G. Dresselhaus, E. P. Ippen, T. Venkatesan, X. D. Wu, and A. Inam, Solid State Commun. **74**, 1305 (1990); J. M. Chwalek, C. Uher, J. F. Whitaker, G. A. Mourou, J. Agostinelli, and M. Lelental, Appl. Phys. Lett. **57**, 1696 (1990).

[18]M. Garriga, U. Venkateswaran, K. Syassen, J. Humlicek, M. Cardona, H. Mattausch, and L. Schonherr, Physica C **153-155**, 643 (1988); J. Kircher, M. K. Kelly, S. Rashkeev, M. Alouani, D. Fuchs, and M. Cardona, Phys. Rev. B **44**, 217 (1991); H. Yasuoka, H. Mazaki, T. Terashima, and Y. Bando, Physica C **175**, 192 (1991).

[19]For example, see J. M. Tranquada, in *Earlier and Recent Aspects of Superconductivity,* edited by J. G. Bednorz and K. A. Muller, Vol. 90 of *Springer Series in Solid State Science* (Springer-Verlag Berlin, 1990), p. 422.

[20]P. Dougier and A. Casalot, J. Solid State Chem. **2**, 396 (1970); P. Dougier, Ph.D thesis, University of Bordeaux, 1975.

[21]N. F. Mott, Adv. Phys. **39**, 61 (1990).

[22]P. W. Anderson, Phys. Rev. **109**, 1492 (1958); **109**, 1972 (1958); Proc. Nat. Acad. Sci. (USA) **69**, 1097 (1985).

[23](a) N. F. Mott and E. A. Davis, *Electronic Processes in Noncrystalline Materials* (Claredon, Oxford, 1979), Chap. 4; (b) N. F. Mott, Adv. Phys. **34**, 329 (1985).

[24]A. F. Ioffe and A. R. Regel, Prog. Semicond. **4**, 237 (1960).

[25]D. C. Licciardello and D. J. Thouless, J. Phys. C **8**, 4157 (1975).

[26]G. Yu *et al.* (unpublished). The spectral response of the photoconductivities in $YBa_2Cu_3O_{7-\delta}$ show that in $YBa_2Cu_3O_{6.3}$ both the midinfrared and the 1.7-eV absorption features become weakly photoconductive.

[27]N. F. Mott, in *Electronic Processes in Noncrystalline Materials* [Ref. 23 (a)], Sec. 4.2, p. 110.

[28]V. J. Emery, S. A. Kivelson, and H. Q. Lin, Phys. Rev. Lett. **64**, 475 (1990).

[29]V. J. Emery and S. A. Kivelson (private communication).

[30]M. Grilli, R. Raimondi, C. Castellani, C. DiCastro, and G. Kotliar, Phys. Rev. Lett. **67**, 259 (1991).

[31]C. A. Neugebauer and M. B. Webb, J. Appl. Phys. **33**, 74 (1962); R. M. Hill, Proc. R. Soc. London, Ser. A **309**, 377 (1969); C. A. Neugebauer, Thin Solid Films **6**, 443 (1970).

[32]C. M. Foster, A. J. Heeger, Y. H. Kim, G. Stucky, and N. Herron, Synth. Met. **33**, 171 (1989), and references therein; C. M. Foster, Ph.D. thesis, University of California, Santa Barbara, 1990.

[33]D. Mihailovic, C. M. Foster, K. F. Voss, T. Mertelj, I. Poberaj, and N. Herron, Phys. Rev. B **44**, 237 (1991).

[34]B. Batlogg, Physica B, **169**, 7 (1991).

[35]G. Yu, C. H. Lee, A. J. Heeger, S.-W. Cheong, and Z. Fisk Physica C (to be published).

[36]H. Sher *et al.*, Phys. Today **44** (1), 26 (1991), and references therein.